

BI-LoRA: EFFICIENT SHARPNESS-AWARE MINIMIZATION FOR FINE-TUNING LARGE-SCALE MODELS

Yuhang Liu,^{*} Tao Li,^{*} Zhehao Huang, Zuopeng Yang, Xiaolin Huang[†]
Shanghai Jiao Tong University

ABSTRACT

Fine-tuning large-scale pre-trained models with limited data presents significant challenges for generalization. While Sharpness-Aware Minimization (SAM) has proven effective in improving generalization by seeking flat minima, its substantial extra memory and computation overhead make it impractical for large models. Integrating SAM with parameter-efficient fine-tuning methods like Low-Rank Adaptation (LoRA) is a promising direction. However, we find that directly applying SAM to LoRA parameters limits the sharpness optimization to a restricted subspace, hindering its effectiveness. To address this limitation, we propose **Bi-directional Low-Rank Adaptation (Bi-LoRA)**, which introduces an auxiliary LoRA module to model SAM’s adversarial weight perturbations. It decouples SAM’s weight perturbations from LoRA optimization: the primary LoRA module adapts to specific tasks via standard gradient descent, while the auxiliary module captures the sharpness of the loss landscape through gradient ascent. Such dual-module design enables Bi-LoRA to capture broader sharpness for achieving flatter minima while remaining memory-efficient. Another important benefit is that the dual design allows for simultaneous optimization and perturbation, eliminating SAM’s doubled training costs. Extensive experiments across diverse tasks and architectures demonstrate Bi-LoRA’s efficiency and effectiveness in enhancing generalization.

1 INTRODUCTION

The paradigm of pretraining followed by fine-tuning has become the de facto standard in machine learning, demonstrating state-of-the-art performance across various tasks (Devlin et al., 2018; Kolesnikov et al., 2020; Dosovitskiy et al., 2021; Radford et al., 2021). However, as model sizes continue to grow, fine-tuning with limited data presents significant challenges for generalization. In such scenarios, the risk of overfitting becomes particularly acute and can significantly compromise model performance.

Motivated by the connection between flatness of the loss landscape and generalization, one promising direction for improving generalization is to seek flat minima (Hochreiter & Schmidhuber, 1994; 1997). Sharpness-Aware Minimization (SAM) (Foret et al., 2021) is a widely used technique that enhances generalization by formulating optimization as a min-max problem, effectively minimizing the worst-case loss within a local neighborhood. It has achieved state-of-the-art performance in small-scale training scenarios (Chen et al., 2022; Zhuang et al., 2022). However, SAM requires calculating an adversarial perturbation of model parameters at each training step, incurring additional memory overhead of a copy of the model weights and doubling the training time. When applied to large-scale models, the cost in memory and computation becomes particularly significant.

A very successful approach for reducing memory cost in large-scale model training is Low-Rank Adaptation (LoRA) (Hu et al., 2022), which introduces trainable, task-specific low-rank matrices to model weight updates. LoRA greatly lowers memory requirements by significantly cutting the trainable parameters and has become one of the most popular solutions for fine-tuning and deploying large models due to its simplicity and performance comparable to full fine-tuning (Full FT).

^{*}Equal contribution.

[†]Corresponding author.

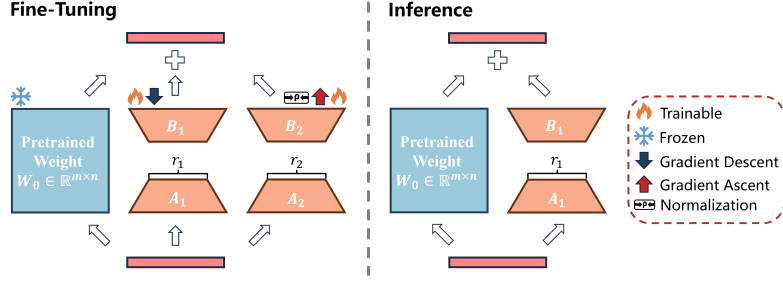


Figure 1: An overview of our proposed Bi-LoRA. During fine-tuning (**Left**), Bi-LoRA utilizes two LoRA modules: the primary LoRA module ($B_1 A_1$) is optimized by gradient descent for task-specific adaptation, while the auxiliary LoRA module ($B_2 A_2$) performs gradient ascent to inject norm-constrained adversarial perturbations simultaneously. At inference (**Right**), only the ($B_1 A_1$) is retained and merged with the pretrained weights; ($B_2 A_2$) is discarded.

Naturally, one could seek flat minima for large models while maintaining memory efficiency by applying SAM to LoRA parameters, referred to as LoRA-SAM (Li et al., 2024a). However, we find that this straightforward integration encounters an essential mismatch: the forward inference is working in the whole parameter space and thus cares about the sharpness of the whole space, while LoRA-SAM imposes adversarial directions on the reduced space and can only capture the sharpness therein. In other words, LoRA-SAM optimizes flatness in the restricted subspace, which is not necessarily also flat in the full parameter space.

To deal with this inconsistency, we propose to introduce an auxiliary LoRA module to model broader perturbations. During training, while the primary LoRA module undergoes gradient descent as in standard LoRA optimization, the auxiliary LoRA module performs gradient ascent to simulate SAM’s adversarial perturbations. We term our approach **Bi-directional Low-Rank Adaptation** (Bi-LoRA). Compared to LoRA-SAM, the bi-directional module design separates optimization and perturbation subspaces, enabling the training to capture broader sharpness beyond the restricted subspace and promote flatter minima. Because both modules are updated in a single backward pass, Bi-LoRA preserves the training efficiency of LoRA while eliminating SAM’s extra compute and significantly improving generalization, making it a favorable alternative for fine-tuning large-scale models.

Our contributions can be summarized as follows:

- We reveal that directly applying SAM to LoRA parameters can only optimize the sharpness of the loss landscape within the “restricted subspace” (see Proposition 3.1 for more formal definition), thereby limiting its potential to improve generalization.
- We propose **Bi-LoRA**, which introduces an auxiliary LoRA module to model SAM’s adversarial weight perturbation, decoupling it from LoRA optimization. This design enables simultaneous optimization of SAM’s two steps with minor additional memory costs.
- Extensive experiments across a wide range of fine-tuning tasks—including natural language understanding, mathematics, code generation, chat, instruction following, and diffusion models—demonstrate that Bi-LoRA achieves superior generalization performance.

2 RELATED WORK

Low-Rank Adaptation (LoRA). LoRA (Hu et al., 2022) is a widely adopted parameter-efficient fine-tuning (PEFT) method. It models weight updates via low-rank matrices without incurring additional inference costs. Many studies have been proposed to improve the performance of LoRA (Koochpayegani et al., 2024; Dou et al., 2024; Tian et al., 2024; Wang et al., 2025; Yen et al., 2025; Wu et al., 2025). On the resource perspective, AdaLoRA (Zhang et al., 2023) dynamically adjusts the rank allocation, while MELoRA (Ren et al., 2024) trains multiple mini-LoRA modules in parallel to cut down on trainable parameters. From the optimization perspective, LoRA-GA (Wang et al., 2024), PISSA (Meng et al., 2024) and MiLoRA (Zhang et al., 2024) accelerate convergence and boost performance through enhanced initialization, and DoRA (Liu et al., 2024) decomposes the adaptation into magnitude and direction for better optimization. In this paper, we enhance LoRA optimization

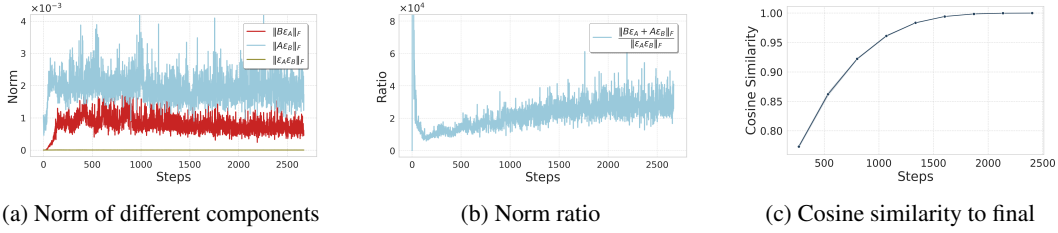


Figure 2: Training statistics for LoRA-SAM. (a) and (b): Frobenius norms of different terms and the ratio of the Frobenius norms of $(B\epsilon_A + \epsilon_B A)$ to that of $(\epsilon_B\epsilon_A)$ in Eqn. (5) during fine-tuning. We monitor a fixed LoRA module (e.g., the query of attention layer in the 7th encoder block; more similar experiments can be found in Appendix J). The norm of the third term $(\epsilon_B\epsilon_A)$ is several orders of magnitude ($> 10^4$) smaller than that of the first two terms, making it negligible. Note that $\|B\epsilon_A\|_F$ is initially zero since B are initialized to zero by default (Hu et al., 2022). (c): Cosine similarity between the final LoRA parameters and those during fine-tuning. The LoRA parameters converge rapidly during fine-tuning. The experiments are conducted on CoLA with the T5-base model.

by optimizing the loss landscape sharpness of the full parameter space through an auxiliary LoRA module. Our approach is orthogonal to prior works.

Sharpness-Aware Minimization (SAM). SAM formulates the optimization objective as a min-max problem to seek flat minima, encouraging model parameters to reside in regions with consistently low loss values, yielding state-of-the-art generalization and robustness. Despite its effectiveness, SAM doubles the computational cost because its inner maximization is approximated via an additional gradient ascent step, thereby limiting its application to large-scale models. Several SAM variants have been developed to enhance its generalization performance (Kim et al., 2022; Li & Giannakis, 2023; Li et al., 2024c). ASAM (Kwon et al., 2021) introduces adaptive sharpness to address SAM’s scale-dependency issue, while GSAM (Zhuang et al., 2022) jointly minimizes surrogate and perturbed losses to locate flatter region. Meanwhile, other works aim to improve SAM’s training efficiency (Du et al., 2022; Jiang et al., 2023; Ji et al., 2024). LookSAM (Liu et al., 2022) applies adversarial perturbations only periodically. Recent studies have also focused on applying SAM to LoRA fine-tuning, aiming to enhance generalization while maintaining training efficiency. For example, BAR (Li et al., 2024a) makes SAM’s implicit balancedness regularization explicit for scale-invariant tasks like LoRA, achieving SAM-level generalization gains with significantly less computation. Flat-LoRA (Li et al., 2024b) replaces the costly inner maximization with random weight perturbation to tackle the coupling issue in LoRA-SAM without sacrificing efficiency. In this paper, we introduce a novel framework that integrates SAM with LoRA through dual LoRA modules. Our method employs auxiliary LoRA modules to generate adversarial perturbations decoupled from optimization, incurring minimal additional overhead.

3 ISSUES OF LORA-SAM

3.1 PRELIMINARIES

Given a pre-trained weight matrix $W_0 \in \mathbb{R}^{m \times n}$, LoRA utilizes low-rank matrices B and A to model the weight change ΔW during the fine-tuning,

$$W = W_0 + \Delta W \approx W_0 + BA, \quad (1)$$

where $B \in \mathbb{R}^{m \times r}$ and $A \in \mathbb{R}^{r \times n}$ with $r \ll \min\{m, n\}$. Here we omit the scaling factor $s = \alpha/r$ for the sake of simplicity in the equation, as it can be easily incorporated into B and A .

During gradient back-propagation, the loss gradient w.r.t. B and A is computed using the chain rule:

$$\frac{\partial \mathcal{L}}{\partial B} = (\nabla_W \mathcal{L}) A^\top, \quad \frac{\partial \mathcal{L}}{\partial A} = B^\top (\nabla_W \mathcal{L}), \quad (2)$$

where \mathcal{L} is the loss objective to be minimized.

3.2 LoRA-SAM

For optimizing the sharpness while keeping memory efficiency, a natural idea is to apply SAM over the LoRA parameters (LoRA-SAM) which formulates the following optimization target:

$$\min_{B,A} \max_{\|(\epsilon_B, \epsilon_A)\| \leq \rho} \mathcal{L}(W_0 + (B + \epsilon_B)(A + \epsilon_A)), \quad (3)$$

where $\epsilon_B \in \mathbb{R}^{m \times r}$, $\epsilon_A \in \mathbb{R}^{r \times n}$ are the adversarial weight perturbations over low-rank matrices, $\|(\epsilon_B, \epsilon_A)\|$ denotes the norm of weight perturbations (a typical setting is the ℓ_2 -norm), and ρ is the neighborhood radius.

To efficiently solve the inner maximization problem in Eqn. (3), Foret et al. (2021) employ first-order Taylor expansion for approximation, and the resulting perturbations are calculated as follows:

$$\epsilon_B = \rho \cdot \frac{\partial \mathcal{L}}{\partial B} / F_{\text{total}}, \quad \epsilon_A = \rho \cdot \frac{\partial \mathcal{L}}{\partial A} / F_{\text{total}}, \quad F_{\text{total}} = \sqrt{\left\| \frac{\partial \mathcal{L}}{\partial B} \right\|_F^2 + \left\| \frac{\partial \mathcal{L}}{\partial A} \right\|_F^2}, \quad (4)$$

where $\|\cdot\|_F$ denotes the Frobenius norm. Then we can rewrite perturbation given by Eqn. (3) as

$$\epsilon_W = B\epsilon_A + \epsilon_B A + \epsilon_B \epsilon_A. \quad (5)$$

Since both ϵ_A and ϵ_B are several orders of magnitude smaller than the original matrices A and B , the cross term $\epsilon_B \epsilon_A$ is negligible, as evidenced by Figures 2a and 2b, which report the magnitudes of these terms. Therefore, Eqn. (5) can be approximately simplified as:

$$\epsilon_W \approx c [BB^\top (\nabla_W \mathcal{L}) + (\nabla_W \mathcal{L}) A^\top A], \quad (6)$$

where $c = \rho / \sqrt{\|(\nabla_W \mathcal{L}) A^\top\|_F^2 + \|B^\top (\nabla_W \mathcal{L})\|_F^2}$. Now one can see the perturbation of LoRA-SAM is confined to a restricted subspace, as demonstrated below:

Proposition 3.1 (Perturbation Space of LoRA-SAM). *The effective weight perturbation in LoRA-SAM can be decomposed into two terms: $BB^\top (\nabla_W \mathcal{L})$ and $(\nabla_W \mathcal{L}) A^\top A$. The column space of the first term is given by $\text{Col}(B)$, while the row space of the second term is given by $\text{Row}(A)$.*

The space for adversarial weight perturbation in LoRA-SAM is primarily dominated by $\text{Col}(B)$ and $\text{Row}(A)$, from which it follows that LoRA-SAM only cares about the sharpness within the subspace defined by B and A , failing to capture the sharpness in a broader space.

Moreover, as training progresses, B and A would converge rapidly, as demonstrated in Figure 2c. This results in a corresponding convergence of the column and row spaces $\text{Col}(B)$ and $\text{Row}(A)$, further restricting the subspace for sharpness optimization and hindering the effectiveness of LoRA-SAM, potentially leading to suboptimal performance.

In Figure 3, we compare the loss landscape flatness of different methods. We observe that LoRA-SAM achieves the flattest loss landscape within the LoRA parameter space as in Figure 3a, reflecting its original sharpness-minimization objective. In contrast, Figure 3b shows that while LoRA-SAM yields a flatter landscape than LoRA in the full space, the loss still rises sharply with perturbation magnitude. This indicates the limitation of applying perturbation in a restricted subspace, highlighting the importance of considering sharpness over a broader space beyond LoRA subspace.

4 BI-LoRA: BI-DIRECTIONAL LOW-RANK ADAPTATION

In this section, we introduce Bi-LoRA, a novel dual-LoRA architecture that utilizes decoupled LoRA modules to separately model LoRA optimization and SAM perturbation, enhancing the effectiveness of generalization improvement for large models while preserving training efficiency.

The primary limitation of LoRA-SAM is that the spaces for LoRA optimization and SAM’s adversarial weight perturbation are coupled, as discussed in Proposition 3.1, which undermines the effectiveness of sharpness optimization. To address this limitation, we propose to decouple the spaces for these two operations. Specifically, we introduce two separated LoRA modules to model them, respectively:

$$W = W_0 + B_1 A_1 + B_2 A_2, \quad (7)$$

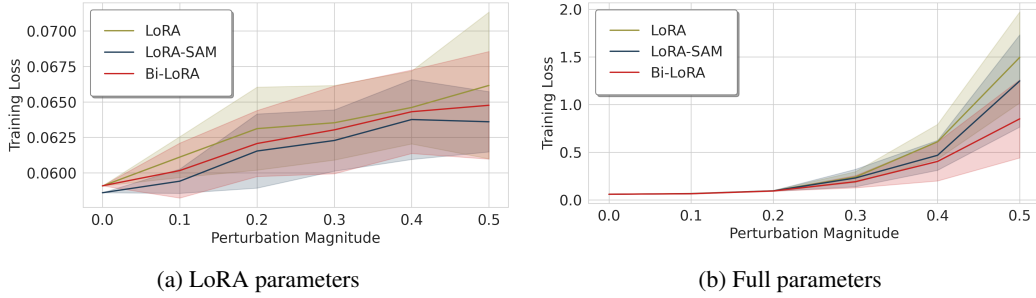


Figure 3: Loss landscape visualization along a normalized random direction using the technique proposed by Li et al. (2018), with (a) focusing on LoRA parameters and (b) on full parameters excluding the LoRA modules. All experiments are independently repeated five times using the T5-base model fine-tuned on the CoLA dataset. It could be observed that LoRA-SAM and Bi-LoRA both achieve better flatness compared to vanilla LoRA. (a) In the LoRA parameter space, LoRA-SAM achieves the best flatness, as expected from its sharpness-minimization objective in LoRA subspace. (b) reveals that LoRA-SAM may have sharp training loss increase as perturbation in the full parameter space. By contrast, the proposed Bi-LoRA method delivers a markedly larger flatness gain than LoRA-SAM in the full parameter space.

where the first LoRA module, i.e., $B_1 A_1$, serves as the primary module responsible for task-specific adaptation, similar to standard LoRA, while the second module $B_2 A_2$ acts as the auxiliary LoRA module for modeling adversarial perturbation in SAM.

With these two modules, the Bi-LoRA’s optimization objective is given below,

$$\min_{B_1, A_1} \max_{\|B_2 A_2\|_F \leq \rho} \mathcal{L}(W_0 + B_1 A_1 + B_2 A_2), \quad (8)$$

where $\rho > 0$ is the neighborhood radius that controls the magnitude of perturbations as in the original SAM. Compared to the LoRA-SAM’s objective in Eqn. (3), we use an independent auxiliary module to directly model the perturbation, thereby eliminating the dependence on the primary LoRA module.

Then we can conclude the properties of weight perturbation for Bi-LoRA as follows:

Proposition 4.1 (Perturbation space of Bi-LoRA). *The column space for the weight perturbation in Bi-LoRA is spanned by $\text{Col}(B_2)$, which is independent of the LoRA optimization space, i.e., $\text{Col}(B_1)$.*

Although Bi-LoRA’s perturbation space $\text{Col}(B_2)$ (auxiliary) remains a subspace, it is strictly decoupled from the optimization space $\text{Col}(B_1)$ (primary). The auxiliary modules converge *much more slowly* than the primary ones, preserving flexibility for sharpness-aware updates (see Appendix C). Furthermore, we will show in Section 5.7 that increasing the auxiliary rank from 0 to 8 consistently improves performance. Therefore, Bi-LoRA enables a more effective captures of sharpness in the full parameter space. And Figure 3 confirms that Bi-LoRA achieves a significantly flatter loss landscape both in the LoRA parameter space and the full parameter space, leading to improved generalization.

Efficient optimization. Decoupling the training and the perturbation in Eqn. (8) enables an efficient optimization strategy for Bi-LoRA: one can simultaneously perform LoRA optimization and sharpness-aware minimization *in one gradient step*. Specifically, during each iteration, the primary LoRA module ($B_1 A_1$) is updated through standard gradient descent, while the auxiliary LoRA module ($B_2 A_2$) is updated through gradient ascent for sharpness optimization. The bi-directional gradient update approach embodies the core concept of our method, which we designate as **Bi-directional Low-Rank Adaptation (Bi-LoRA)**. Concretely, one update step for Bi-LoRA is formalized as follows:

$$\begin{cases} B_1^{k+1} = B_1^k - \eta_1 (\nabla_W \mathcal{L}) A_1^{k\top}, & A_1^{k+1} = A_1^k - \eta_1 B_1^{k\top} (\nabla_W \mathcal{L}), \\ B_2^{k+1} = B_2^k + \eta_2 (\nabla_W \mathcal{L}) A_2^{k\top}, & A_2^{k+1} = A_2^k + \eta_2 B_2^{k\top} (\nabla_W \mathcal{L}), \end{cases} \quad (9)$$

where $\nabla_W \mathcal{L} = \frac{\partial \mathcal{L}}{\partial W} \Big|_{W=W_0+B_1^k A_1^k+B_2^k A_2^k}$ is the gradient of the loss \mathcal{L} w.r.t. the merged weight W , k denotes the iteration index, and η_1, η_2 are learning rates. We use the same learning rate for both LoRA modules in our experiments, though other choices are possible (see Appendix G). Note that the two LoRA modules are optimized jointly, and the steps in Eqn. (9) can be performed in a single gradient backpropagation. This eliminates the doubled computational cost typically incurred by LoRA-SAM.

Algorithm 1 Bi-LoRA

```
1: Input: Initial weight  $W_0$ , learning rates  $\eta_1, \eta_2$ , radius  $\rho$ , number of LoRA layers  $N$ 
2: Output: Adapted weight  $W$  for inference
3: Initialize LoRA modules  $B_1^0, A_1^0, B_2^0, A_2^0$ ;
4:  $k \leftarrow 0$ ;
5: while not converged do
6:   Sample mini-batch data  $\mathcal{B}$ ;
7:   Apply gradient descent to primary and ascent to auxiliary LoRA modules via Eqn. (9);
8:   Clip the auxiliary modules via Eqn. (10);
9:    $k \leftarrow k + 1$ ;
10: end while
11: Remove the auxiliary LoRA modules  $B_2^k, A_2^k$ ;
12: return  $W^k = W_0 + B_1^k A_1^k$ 
```

Norm constraint. In the above, we describe the training scheme for Bi-LoRA that simultaneously optimizes the two LoRA modules for efficient sharpness-aware minimization. One remaining consideration is the norm constraint in Eqn. (8), which ensures the perturbation remains sufficiently small to avoid disrupting normal model training.

To maintain the weight perturbation within a controlled magnitude, we propose to clip the auxiliary module ($B_2 A_2$) after each update, based on their total Frobenius norm. Specifically, suppose that there are N LoRA layers. The i -th auxiliary module is scaled as follows:

$$\begin{cases} B_2^{(i)} \leftarrow \sqrt{\rho/c_{\text{norm}}} \cdot B_2^{(i)}, \\ A_2^{(i)} \leftarrow \sqrt{\rho/c_{\text{norm}}} \cdot A_2^{(i)}, \end{cases} \quad \text{if } c_{\text{norm}} > \rho. \quad (10)$$

The normalization is applied only if the total Frobenius norm over N auxiliary LoRA modules c_{norm} exceeds the neighborhood radius ρ , where $c_{\text{norm}} = \sqrt{\sum_{j=1}^N \|B_2^{(j)} A_2^{(j)}\|_F^2}$. This ensures the perturbation remains constrained within the preset ρ -norm ball.

Inference. After training, we discard the auxiliary modules ($B_2 A_2$), as they serve solely to optimize sharpness during training and guide the primary module ($B_1 A_1$) towards a flat region. Consequently, the adapted weights are reduced to the primary module, i.e., $W = W_0 + B_1 A_1$, preserving the original LoRA structure and ensuring no additional computational overhead during inference.

The procedure for Bi-LoRA is summarized in Algorithm 1.

5 EXPERIMENTS

In this section, we evaluate the performance of Bi-LoRA across diverse benchmark tasks. We begin with natural language understanding tasks, including GLUE (Wang et al., 2019b) and Super-GLUE (Wang et al., 2019a), using the T5-base model (Raffel et al., 2020). Next, we test its capabilities in mathematical reasoning, code generation, dialogue generation, and instruction-following tasks using the Llama 2/3.1 models (Touvron et al., 2023; Dubey et al., 2024). Additionally, we assess Bi-LoRA’s effectiveness on diffusion models and conduct ablation studies.

Table 1: Results on fine-tuning the T5-base model on a subset of GLUE datasets. “Cost” indicates the gradient steps per training iteration, e.g., one step (Cost $\times 1$) for Full FT, LoRA, and Bi-LoRA.

Dataset Size	Cost	MNLI (393k)	SST2 (67k)	CoLA (8.6k)	QNLI (105k)	MRPC (3.7k)	Avg.
Full FT	$\times 1$	85.57 \pm 0.09	94.27 \pm 0.24	56.60 \pm 0.62	93.18 \pm 0.09	87.30 \pm 0.79	83.38
LoRA	$\times 1$	86.25 \pm 0.16	94.23 \pm 0.30	59.41 \pm 0.52	93.25 \pm 0.06	88.56 \pm 0.26	84.34
LoRA-SAM	$\times 2$	86.25 \pm 0.09	94.46 \pm 0.17	59.80 \pm 0.85	93.21 \pm 0.16	88.73 \pm 0.52	84.49
Bi-LoRA	$\times 1$	86.33 \pm 0.08	94.34 \pm 0.05	60.77 \pm 0.39	93.25 \pm 0.06	89.38 \pm 0.26	84.81

Table 2: Results on fine-tuning T5-base with a subset of SuperGLUE datasets. “Cost” indicates the gradient steps per training iteration, e.g., one step (Cost \times 1) for Full FT, LoRA, and Bi-LoRA.

Dataset Size	Cost	BoolQ (9.4k)	CB (0.25k)	COPA (0.4k)	RTE (2.5k)	WIC (5.4k)	Avg.
Full FT	$\times 1$	72.19 \pm 0.14	92.26 \pm 0.24	64.67 \pm 0.26	84.48 \pm 0.12	68.34 \pm 0.19	76.39
LoRA	$\times 1$	72.20 \pm 0.21	92.86 \pm 0.27	63.80 \pm 0.23	83.10 \pm 0.29	68.60 \pm 0.32	76.11
LoRA-SAM	$\times 2$	72.47 \pm 0.42	92.32 \pm 0.28	64.20 \pm 0.42	83.47 \pm 0.47	68.55 \pm 0.76	76.20
Bi-LoRA	$\times 1$	72.25 \pm 0.30	92.86 \pm 0.32	64.60 \pm 0.25	83.61 \pm 0.37	70.69 \pm 0.40	76.80

5.1 BASELINES

We mainly compare with the following baseline methods:

- **Full FT** fine-tunes all model parameters.
- **LoRA** applies low-rank adaptation to all linear modules.
- **LoRA-SAM** applies sharpness-aware minimization over LoRA parameters.
- **Efficient SAM variants designed for LoRA fine-tuning**, including LoRA-oBAR/nBAR (Li et al., 2024a), and Flat-LoRA (Li et al., 2024b).
- **LoRA variants**, including LoRA-GA (Wang et al., 2024), PiSSA (Meng et al., 2024) and DoRA (Liu et al., 2024).

We tune the neighborhood radius ρ over $\{0.005, 0.01, 0.05, 0.1, 0.2, 0.5\}$ for LoRA-SAM and Bi-LoRA and search learning rates among $\{2e-5, 5e-5, 1e-4, 2e-4\}$ for Full FT and $\{5e-5, 1e-4, 2e-4, 5e-4, 1e-3\}$ for LoRA and its variants. To more rigorously evaluate the effectiveness in improving generalization, we adopt a stronger training protocol than prior works (Wang et al., 2025; 2024). The same protocol is applied across all methods for fairness. Unless otherwise stated, all results are averaged over three independent runs with standard errors. See Appendix H for more training details.

5.2 RESULTS ON NATURAL LANGUAGE UNDERSTANDING

Setting. We fine-tune the T5-base model on multiple datasets from GLUE and SuperGLUE benchmarks, including MNLI, SST2, CoLA, QNLI, MRPC, BoolQ, CB, COPA, RTE, and WIC, following Wang et al. (2024); Li et al. (2024b). Performance is evaluated on the development set using accuracy as the primary metric, except for CoLA, where the Matthews correlation coefficient is used.

Results. We first focus on the GLUE datasets. From the results in Table 1, we observe that Bi-LoRA outperforms both LoRA and LoRA-SAM, achieving an average improvement of 0.47% and 0.32%, respectively. It is worth noting that Bi-LoRA achieves these gains with the same training speed as LoRA, whereas LoRA-SAM doubles the training time. Moreover, the gains are more pronounced on smaller datasets, with Bi-LoRA outperforming LoRA by 1.36% on CoLA and 0.82% on MRPC. In contrast, LoRA-SAM shows no clear advantage over vanilla LoRA, indicating its limited ability to enhance generalization due to constrained sharpness optimization.

Next, we evaluate on the SuperGLUE datasets, which feature more challenging language understanding tasks. To reduce variance from the limited evaluation sizes of CB (56), COPA (100), and RTE (277) samples, we increase the number of runs from 3 to 20 for CB and COPA, and to 5 for RTE. Table 2 shows Bi-LoRA demonstrates more significant advantages over LoRA and LoRA-SAM by 0.69% and 0.60% on average, while LoRA-SAM yields minimal gains and even hurts some datasets (e.g., CB). These results confirm the effectiveness of Bi-LoRA in enhancing generalization.

5.3 RESULTS ON LARGE LANGUAGE MODELS

Setting. We evaluate the performance of Bi-LoRA on Llama 2-7B/3.1-8B across four tasks: mathematical reasoning, code generation, dialogue generation, and instruction following, following Wang et al. (2024); Li et al. (2024b); Ren et al. (2024). Llama 2-7B is fine-tuned on the first three tasks, while Llama 3.1-8B is used for instruction following. Each task focuses on a specific capability and uses well-established datasets and metrics for training and evaluation, as detailed below:

- **Mathematical reasoning.** Our model is fine-tuned on a 100k subset of MetaMathQA and evaluated on GSM8K. Performance is measured by accuracy.

Table 3: Results of fine-tuning Llama 2-7B and Llama 3.1-8B on different tasks. “Cost” indicates the gradient steps per training iteration, e.g., one step (Cost \times 1) for Full FT, LoRA, and Bi-LoRA.

Method	Cost	Llama 2-7B			Llama 3.1-8B			
		GSM8K	HumanEval	MT-Bench	MMLU	DROP	HEval	BBH
Full FT	$\times 1$	59.74 \pm 0.69	33.12 \pm 0.32	6.16 \pm 0.09	64.31 \pm 0.31	51.52 \pm 0.45	41.45 \pm 1.58	44.78 \pm 0.33
LoRA	$\times 1$	58.21 \pm 0.34	24.75 \pm 0.23	6.08 \pm 0.11	63.38 \pm 0.39	49.82 \pm 0.54	43.15 \pm 0.93	42.82 \pm 0.27
LoRA-SAM	$\times 2$	59.16 \pm 0.52	26.59 \pm 0.36	5.82 \pm 0.07	63.46 \pm 0.19	50.94 \pm 0.22	44.36 \pm 1.13	43.49 \pm 0.40
Bi-LoRA	$\times 1$	60.32 \pm 0.30	27.20 \pm 0.42	6.24 \pm 0.05	63.67 \pm 0.15	51.53 \pm 0.33	46.12 \pm 0.89	43.45 \pm 0.31

- **Code generation.** We fine-tune our model on a 100k subset of Code-Feedback and evaluate it on the HumanEval benchmark, using the PASS@1 metric.
- **Dialogue generation.** We train our model on the WizardLM dataset and evaluate it on MT-Bench. The response quality is assessed with GPT-4, and we report the first-turn score on a 10-point scale.
- **Instruction following.** Fine-tuned on Cleaned Alpaca (Taori et al., 2023) and evaluated on INSTRUCTEVAL (Chia et al., 2023), reporting exact match for MMLU, DROP, and BBH, and PASS@1 for HumanEval.

Results. We begin by focusing on Llama 2-7B for math, code, and chat tasks. The results, presented in Table 3, demonstrate Bi-LoRA’s superior performance. Compared to LoRA, Bi-LoRA achieves improvements of 2.11% accuracy on GSM8K, 2.45% on HumanEval, and 0.16 on MT-Bench. Importantly, these gains are even more pronounced than those achieved with the smaller T5-base model, and Bi-LoRA operates at a similar speed as LoRA, underscoring its scalability. Furthermore, Bi-LoRA narrows the gap between LoRA fine-tuning and full fine-tuning, and notably outperforms full fine-tuning on GSM8K and MT-Bench tasks, which are not attainable by competing methods. In contrast, we observe that LoRA-SAM does not consistently improve upon LoRA.

Next, we turn our attention to the instruction following task with the Llama 3.1-8B model. As shown in Table 3, Bi-LoRA consistently outperforms baseline methods, surpassing LoRA by 0.29% on MMLU, 1.71% on DROP, 2.97% on HumanEval, and 0.63% on BBH. Although LoRA-SAM shows improvements over LoRA, Bi-LoRA achieves more substantial gains, particularly on DROP and HumanEval datasets, while requiring only half the training time.

5.4 RESULTS ON DIFFUSION MODELS

Setting. We apply LoRA to subject-driven generalization task and finetune SDXL (Podell et al., 2023) via Dreambooth (Ruiz et al., 2023) on 23-image 3D Icons dataset.

Results. Table 4 reports the average CLIP image-text (I2T) and text-text (T2T) similarity scores over 200 prompts of the form “*a ToK icon of a <Instance>, in the style of TOK.*” Bi-LoRA improves I2T similarity on five of six cases, most notably by +2.43% for Roaring Lion, yielding an average gain of 0.70% over vanilla LoRA. T2T similarity gains are even more substantial: Bi-LoRA outperforms LoRA on all instances (up to +6.53% for Roaring Lion), with an average improvement of 3.85%. These results demonstrate that Bi-LoRA both enhances personalization and better preserves textual consistency with the target icon prompt. Qualitative examples are shown in Appendix B.

Table 4: Average CLIP I2T and T2T similarity (%) for LoRA and Bi-LoRA on the 3D Icons dataset over 200 prompts.

Instance	CLIP I2T (\uparrow)		CLIP T2T (\uparrow)	
	LoRA	Bi-LoRA	LoRA	Bi-LoRA
Fluffy Rabbit	32.45	32.84	49.04	51.00
Curly Cloud	32.06	31.99	36.90	42.49
Roaring Lion	30.47	32.90	38.71	45.24
Dripping Water Drop	32.47	33.18	40.55	41.92
Hopping Frog	33.40	33.87	41.12	42.93
Smiling Sun	33.75	34.04	51.31	57.17

5.5 COMPARISON WITH EFFICIENT SAM VARIANTS FOR LoRA FINE-TUNING

In Table 5, we compare Bi-LoRA with three recent efficient SAM variants designed for LoRA, all of which remove SAM’s extra gradient step. Bi-LoRA outperforms LoRA-oBAR/nBAR and Flat-LoRA by 1.89%, 0.78%, and 0.32% on average, respectively. While LoRA-oBAR/nBAR successfully leverage the implicit balancedness regularization of LoRA-SAM and improve the generalization over vanilla LoRA, they may still be limited by the restricted perturbation subspace as in LoRA-SAM. Flat-LoRA employs purely random perturbations in pursuit of flatness in the full parameter space. In

Table 5: Performance on GSM8K and HumanEval for Bi-LoRA and other efficient SAM variants.

Method	GSM8K	HumanEval	Avg.
LoRA	58.21 \pm 0.34	24.75 \pm 0.23	41.48
LoRA-oBAR	59.66 \pm 0.27	24.07 \pm 0.92	41.87
LoRA-nBAR	60.02 \pm 0.12	25.94 \pm 0.35	42.98
Flat-LoRA	60.65 \pm 0.16	26.22 \pm 0.56	43.44
Bi-LoRA	60.32 \pm 0.30	27.20 \pm 0.42	43.76

contrast, Bi-LoRA can attain better overall generalization performance by employing an auxiliary LoRA module that is iteratively refined to more precisely capture sharpness during the training.

5.6 COMPARISON WITH OTHER LORA VARIANTS

In this section, we evaluate Bi-LoRA’s effectiveness when integrated with existing methods using the T5-base model on the MRPC and CoLA datasets, with detailed training settings provided in Appendix H.1. As shown in Table 6, at its best, integrating Bi-LoRA improves the average score across MRPC and CoLA by 1.45%, achieving gains of up to 1.80% on MRPC and 1.83% on CoLA. These results confirm that Bi-LoRA can be seamlessly integrated with previous approaches and deliver consistent improvements.

Table 6: Results of fine-tuning T5-base on MRPC and CoLA using various LoRA variants, both standalone and combined with Bi-LoRA.

Method	MRPC	CoLA	Avg.
LoRA-GA	88.81 \pm 0.47	58.87 \pm 1.00	73.84
PiSSA	88.15 \pm 0.24	58.66 \pm 0.47	73.41
DoRA	88.81 \pm 0.29	59.89 \pm 0.72	74.35
LoRA-GA + Bi-LoRA	89.62 \pm 0.24	60.70 \pm 0.27	75.16
PiSSA + Bi-LoRA	89.95 \pm 0.50	59.77 \pm 0.83	74.86
DoRA + Bi-LoRA	89.54 \pm 0.13	60.77 \pm 0.47	75.16

5.7 HYPERPARAMETER SENSITIVITY

We investigate the hyperparameter sensitivity of Bi-LoRA from two aspects: (1) the rank of the auxiliary LoRA module r_2 , and (2) the neighborhood radius ρ . For r_2 , we fine-tune T5-base and evaluate its performance on the CoLA dataset, experimenting with $r_1 \in \{4, 8, 16\}$ and $r_2 \in \{2, 4, 8, 16, 32, 64\}$. For the neighborhood radius, we evaluate $\rho \in \{0.01, 0.05, 0.1\}$ across three setups: fine-tuning T5-Base on CoLA and SST-2, and fine-tuning LLaMA 2-7B on the math task mentioned in Section 5.3. The impact of ρ will be discussed in Appendix A.

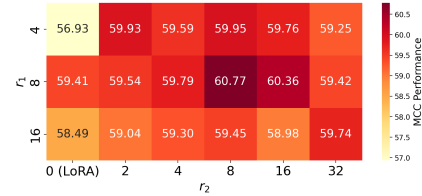


Figure 4: Performance on CoLA under varying ranks of primary (r_1) and auxiliary (r_2) LoRA modules.

Figure 4 shows the performance of Bi-LoRA with varying the primary (r_1) and auxiliary (r_2) LoRA ranks. We observe that integrating the auxiliary module consistently enhances performance. Notably, $r_2 = 8$ generally delivers good results, which we adopt as the default. Additionally, further increasing r_2 does not yield significant improvements.

5.8 TRAINING TIME AND MEMORY COST

We report detailed comparisons of memory and time per optimization step for LoRA, LoRA-SAM and Bi-LoRA on T5-base (CoLA), Llama 2-7B (MetaMathQA), and Llama 3.1-8B (Cleaned Alpaca), spanning NLU, math reasoning, and dialogue.

Table 7 shows that Bi-LoRA significantly reduces the training time cost of LoRA-SAM, decreasing it from over 200% to around 110% relative to base LoRA. This gain comes from jointly performing optimization and perturbation, elim-

Table 7: Peak memory and time per optimization step. Values in parentheses show time relative to LoRA.

Model & Dataset	Method	Memory (GB)	Time (s)
T5-base CoLA	LoRA	3.64	0.27 (100%)
	LoRA-SAM	3.65	0.55 (204%)
	Bi-LoRA	3.68	0.31 (115%)
Llama 2-7B MetaMathQA	LoRA	22.82	4.34 (100%)
	LoRA-SAM	22.87	9.35 (215%)
	Bi-LoRA	23.19	4.50 (104%)
Llama 3.1-8B Cleaned Alpaca	LoRA	25.52	9.49 (100%)
	LoRA-SAM	25.70	19.55 (206%)
	Bi-LoRA	25.88	9.75 (103%)

inating SAM’s extra gradient step In terms of memory, Bi-LoRA incurs only a minimal overhead (e.g., < 0.4GB), as it adds a lightweight auxiliary LoRA module.

6 CONCLUSION

In this paper, we propose Bi-LoRA, a novel dual-LoRA framework that leverages an auxiliary LoRA module to enhance the generalization performance of low-rank adaptation. Bi-LoRA decouples optimization from weight perturbation for better optimizing the sharpness of the loss landscape, allowing both to be updated in a single backward pass without requiring additional gradient steps, as in SAM. Extensive experiments across diverse tasks and architectures demonstrate Bi-LoRA’s efficiency and effectiveness in improving generalization.

REFERENCES

- Xiangning Chen, Cho-Jui Hsieh, and Boqing Gong. When vision transformers outperform resnets without pre-training or strong data augmentations. In *International Conference on Learning Representations (ICLR)*, 2022.
- Yew Ken Chia, Pengfei Hong, Lidong Bing, and Soujanya Poria. Instructeval: Towards holistic evaluation of instruction-tuned large language models. *arXiv preprint arXiv:2306.04757*, 2023.
- Tim Dettmers, Artidoro Pagnoni, Ari Holtzman, and Luke Zettlemoyer. Qlora: Efficient finetuning of quantized llms. In *Advances in Neural Information Processing System (NeurIPS)*, 2023.
- Jacob Devlin, Ming-Wei Chang, Kenton Lee, and Kristina Toutanova. Bert: Pre-training of deep bidirectional transformers for language understanding. *arXiv preprint arXiv:1810.04805*, 2018.
- Alexey Dosovitskiy, Lucas Beyer, Alexander Kolesnikov, Dirk Weissenborn, Xiaohua Zhai, Thomas Unterthiner, Mostafa Dehghani, Matthias Minderer, Georg Heigold, Sylvain Gelly, et al. An image is worth 16x16 words: Transformers for image recognition at scale. In *International Conference on Learning Representations (ICLR)*, 2021.
- Shihan Dou, Enyu Zhou, Yan Liu, Songyang Gao, Wei Shen, Limao Xiong, Yuhao Zhou, Xiao Wang, Zhiheng Xi, Xiaoran Fan, Shiliang Pu, Jiang Zhu, Rui Zheng, Tao Gui, Qi Zhang, and Xuanjing Huang. LoRAMoE: Alleviating world knowledge forgetting in large language models via MoE-style plugin. In *Proceedings of the Association for Computational Linguistics (Volume 1: Long Papers)*, 2024.
- Jiawei Du, Daquan Zhou, Jiashi Feng, Vincent Y. F. Tan, and Joey Tianyi Zhou. Sharpness-aware training for free. In *Advances in Neural Information Processing Systems (NeurIPS)*, 2022.
- Abhimanyu Dubey, Abhinav Jauhri, Abhinav Pandey, Abhishek Kadian, Ahmad Al-Dahle, Aiesha Letman, Akhil Mathur, Alan Schelten, Amy Yang, Angela Fan, et al. The llama 3 herd of models. *arXiv preprint arXiv:2407.21783*, 2024.
- Pierre Foret, Ariel Kleiner, Hossein Mobahi, and Behnam Neyshabur. Sharpness-aware minimization for efficiently improving generalization. In *International Conference on Learning Representations (ICLR)*, 2021.
- Sepp Hochreiter and Jürgen Schmidhuber. Simplifying neural nets by discovering flat minima. In *Advances in Neural Information Processing Systems (NeurIPS)*, 1994.
- Sepp Hochreiter and Jürgen Schmidhuber. Flat minima. *Neural computation*, 1997.
- Edward J. Hu, Yelong Shen, Phillip Wallis, Zeyuan Allen-Zhu, Yanzhi Li, Shean Wang, Lu Wang, and Weizhu Chen. Lora: Low-rank adaptation of large language models. In *International Conference on Learning Representations (ICLR)*, 2022.
- Jie Ji, Gen Li, Jingjing Fu, Fatemeh Afghah, Linke Guo, Xiaoyong Yuan, and Xiaolong Ma. A single-step, sharpness-aware minimization is all you need to achieve efficient and accurate sparse training. In *Advances in Neural Information Processing Systems (NeurIPS)*, 2024.

-
- Weisen Jiang, Hansi Yang, Yu Zhang, and James Kwok. An adaptive policy to employ sharpness-aware minimization. In *The Eleventh International Conference on Learning Representations (ICLR)*, 2023.
- Minyoung Kim, Da Li, Shell X Hu, and Timothy Hospedales. Fisher sam: Information geometry and sharpness aware minimisation. In *International Conference on Machine Learning (ICML)*, 2022.
- Alexander Kolesnikov, Lucas Beyer, Xiaohua Zhai, Joan Puigcerver, Jessica Yung, Sylvain Gelly, and Neil Houlsby. Big transfer (bit): General visual representation learning. In *European conference on computer vision (ECCV)*, 2020.
- Soroush Abbasi Koohpayegani, Navaneet K. L., Parsa Nooralinejad, Soheil Kolouri, and Hamed Pirsiavash. NOLA: compressing lora using linear combination of random basis. In *International Conference on Learning Representations (ICLR)*, 2024.
- Jungmin Kwon, Jeongseop Kim, Hyunseo Park, and In Kwon Choi. ASAM: adaptive sharpness-aware minimization for scale-invariant learning of deep neural networks. In *International Conference on Machine Learning (ICML)*, 2021.
- Bingcong Li and Georgios B. Giannakis. Enhancing sharpness-aware optimization through variance suppression. In *Advances in Neural Information Processing Systems (NeurIPS)*, 2023.
- Bingcong Li, Liang Zhang, and Niao He. Implicit regularization of sharpness-aware minimization for scale-invariant problems. In *Advances in Neural Information Processing Systems (NeurIPS)*, 2024a.
- Hao Li, Zheng Xu, Gavin Taylor, Christoph Studer, and Tom Goldstein. Visualizing the loss landscape of neural nets. In *Advances in Neural Information Processing Systems (NeurIPS)*, 2018.
- Tao Li, Zhengbao He, Yujun Li, Yasheng Wang, Lifeng Shang, and Xiaolin Huang. Flat-lora: Low-rank adaption over a flat loss landscape. In *NeurIPS 2024 Workshop on Fine-Tuning in Modern Machine Learning: Principles and Scalability*, 2024b.
- Tao Li, Pan Zhou, Zhengbao He, Xinwen Cheng, and Xiaolin Huang. Friendly sharpness-aware minimization. In *Proceedings of the IEEE Conference on Computer Vision and Pattern Recognition (CVPR)*, 2024c.
- Shih-Yang Liu, Chien-Yi Wang, Hongxu Yin, Pavlo Molchanov, Yu-Chiang Frank Wang, Kwang-Ting Cheng, and Min-Hung Chen. Dora: Weight-decomposed low-rank adaptation. In *International Conference on Machine Learning (ICML)*, 2024.
- Yong Liu, Siqi Mai, Xiangning Chen, Cho-Jui Hsieh, and Yang You. Towards efficient and scalable sharpness-aware minimization. In *Proceedings of the IEEE Conference on Computer Vision and Pattern Recognition (CVPR)*, 2022.
- Fanxu Meng, Zhaohui Wang, and Muhan Zhang. PiSSA: Principal singular values and singular vectors adaptation of large language models. In *Advances in Neural Information Processing Systems (NeurIPS)*, 2024.
- Dustin Podell, Zion English, Kyle Lacey, Andreas Blattmann, Tim Dockhorn, Jonas Müller, Joe Penna, and Robin Rombach. Sdxl: Improving latent diffusion models for high-resolution image synthesis. *arXiv preprint arXiv:2307.01952*, 2023.
- Alec Radford, Jong Wook Kim, Chris Hallacy, Aditya Ramesh, Gabriel Goh, Sandhini Agarwal, Girish Sastry, Amanda Askell, Pamela Mishkin, Jack Clark, et al. Learning transferable visual models from natural language supervision. In *International Conference on Machine Learning (ICML)*, 2021.
- Colin Raffel, Noam Shazeer, Adam Roberts, Katherine Lee, Sharan Narang, Michael Matena, Yanqi Zhou, Wei Li, and Peter J Liu. Exploring the limits of transfer learning with a unified text-to-text transformer. *Journal of machine learning research (JMLR)*, 2020.

-
- Pengjie Ren, Chengshun Shi, Shiguang Wu, Mengqi Zhang, Zhaochun Ren, Maarten de Rijke, Zhumin Chen, and Jiahuan Pei. Melora: Mini-ensemble low-rank adapters for parameter-efficient fine-tuning. In *Proceedings of the Association for Computational Linguistics (Volume 1: Long Papers)*, 2024.
- Nataniel Ruiz, Yuanzhen Li, Varun Jampani, Yael Pritch, Michael Rubinstein, and Kfir Aberman. Dreambooth: Fine tuning text-to-image diffusion models for subject-driven generation. In *Proceedings of the IEEE Conference on Computer Vision and Pattern Recognition (CVPR)*, 2023.
- Rohan Taori, Ishaan Gulrajani, Tianyi Zhang, Yann Dubois, Xuechen Li, Carlos Guestrin, Percy Liang, and Tatsunori B Hashimoto. Stanford alpaca: An instruction-following llama model, 2023.
- Chunlin Tian, Zhan Shi, Zhijiang Guo, Li Li, and Cheng zhong Xu. HydraloRA: An asymmetric LoRA architecture for efficient fine-tuning. In *Advances in Neural Information Processing Systems (NeurIPS)*, 2024.
- Hugo Touvron, Louis Martin, Kevin Stone, Peter Albert, Amjad Almahairi, Yasmine Babaei, Nikolay Bashlykov, Soumya Batra, Prajjwal Bhargava, Shruti Bhosale, et al. Llama 2: Open foundation and fine-tuned chat models. *arXiv preprint arXiv:2307.09288*, 2023.
- Alex Wang, Yada Pruksachatkun, Nikita Nangia, Amanpreet Singh, Julian Michael, Felix Hill, Omer Levy, and Samuel Bowman. Superglue: A stickier benchmark for general-purpose language understanding systems. In *Advances in Neural Information Processing Systems (NeurIPS)*, volume 32, 2019a.
- Alex Wang, Amanpreet Singh, Julian Michael, Felix Hill, Omer Levy, and Samuel R. Bowman. GLUE: A multi-task benchmark and analysis platform for natural language understanding. In *International Conference on Learning Representations (ICLR)*, 2019b.
- Shaowen Wang, Linxi Yu, and Jian Li. Lora-ga: Low-rank adaptation with gradient approximation. In *Advances in Neural Information Processing Systems (NuerIPS)*, 2024.
- Zhengbo Wang, Jian Liang, Ran He, Zilei Wang, and Tieniu Tan. LoRA-pro: Are low-rank adapters properly optimized? In *International Conference on Learning Representations (ICLR)*, 2025.
- Yichen Wu, Hongming Piao, Long-Kai Huang, Renzhen Wang, Wanhua Li, Hanspeter Pfister, Deyu Meng, Kede Ma, and Ying Wei. SD-loRA: Scalable decoupled low-rank adaptation for class incremental learning. In *International Conference on Learning Representations (ICLR)*, 2025.
- Jui-Nan Yen, Si Si, Zhao Meng, Felix Yu, Sai Surya Duvvuri, Inderjit S Dhillon, Cho-Jui Hsieh, and Sanjiv Kumar. LoRA done RITE: Robust invariant transformation equilibration for loRA optimization. In *International Conference on Learning Representations (ICLR)*, 2025.
- Jingfan Zhang, Yi Zhao, Dan Chen, Xing Tian, Huanran Zheng, and Wei Zhu. Milora: Efficient mixture of low-rank adaptation for large language models fine-tuning. In *Findings of the Association for Computational Linguistics: EMNLP*, 2024.
- Qingru Zhang, Minshuo Chen, Alexander Bukharin, Pengcheng He, Yu Cheng, Weizhu Chen, and Tuo Zhao. Adaptive budget allocation for parameter-efficient fine-tuning. In *International Conference on Learning Representations (ICLR)*, 2023.
- Juntang Zhuang, Boqing Gong, Liangzhe Yuan, Yin Cui, Hartwig Adam, Nicha Dvornek, Sekhar Tatikonda, James Duncan, and Ting Liu. Surrogate gap minimization improves sharpness-aware training. In *International Conference on Learning Representations (ICLR)*, 2022.

APPENDIX

A EFFECT OF THE NEIGHBORHOOD RADIUS ρ

From Table A1, Bi-LoRA performs consistently well across $\rho = \{0.01, 0.05, 0.1\}$, showing its effectiveness to moderate perturbations during training. The ability to achieve strong performance across a range of ρ indicates that Bi-LoRA can effectively adapt to varying levels of perturbation, demonstrating its practicality for diverse applications.

Table A1: Results on CoLA and GSM8K under different values of the neighborhood radius ρ .

ρ	CoLA	GSM8K
0.01	60.15 \pm 0.36	59.36
0.05	60.77 \pm 0.39	59.74
0.10	60.18 \pm 0.59	60.65
0.20	58.95 \pm 0.81	58.83

B QUALITATIVE RESULTS ON SDXL

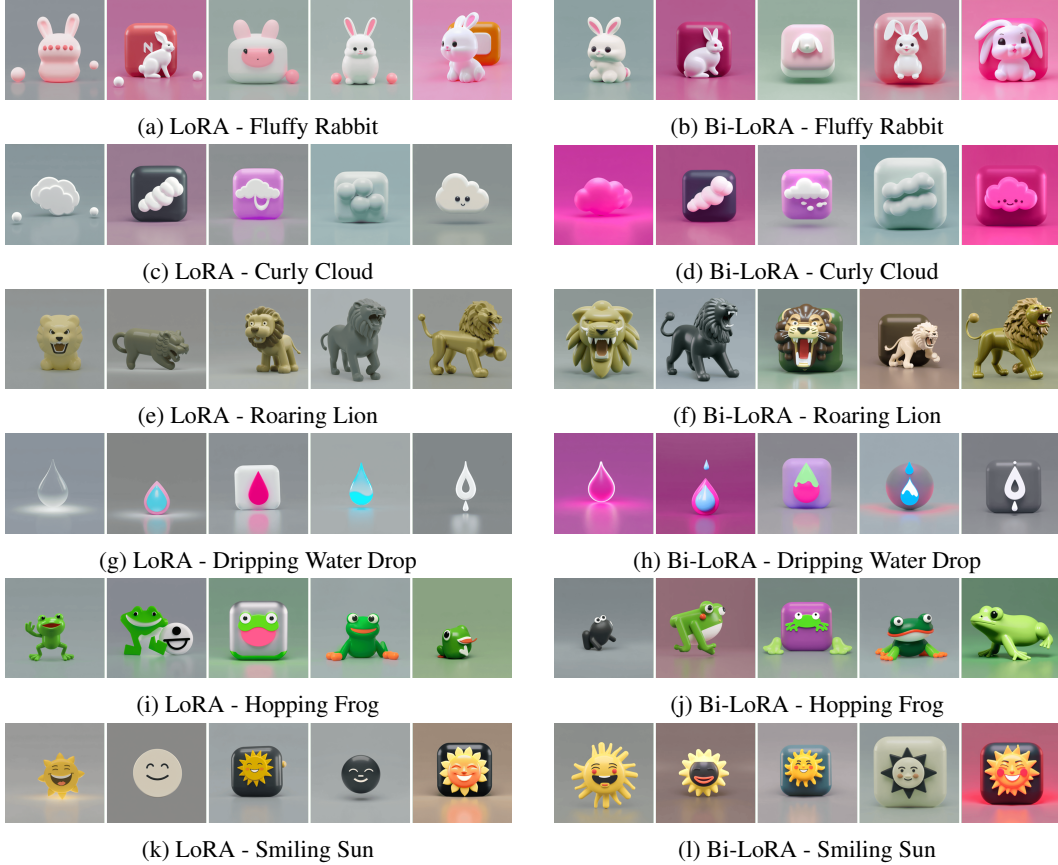


Figure A1: Images generated with SDXL fine-tuned using LoRA (left) and Bi-LoRA (right) on the 3D icon dataset. Each row corresponds to a different prompt in the form “a ToK icon of a <Instance>, in the style of ToK”. Images in the same row are generated with the same random seed for fair comparison.

C CONVERGENCE ANALYSIS OF MAIN AND AUXILIARY LoRA MODULES

We measure the cosine similarity between the weights of the main and auxiliary LoRA modules and their final weights on CoLA and SST2 with T5-base. The results indicate that the auxiliary module converges substantially slower than the main one, preserving flexibility for sharpness-aware updates.

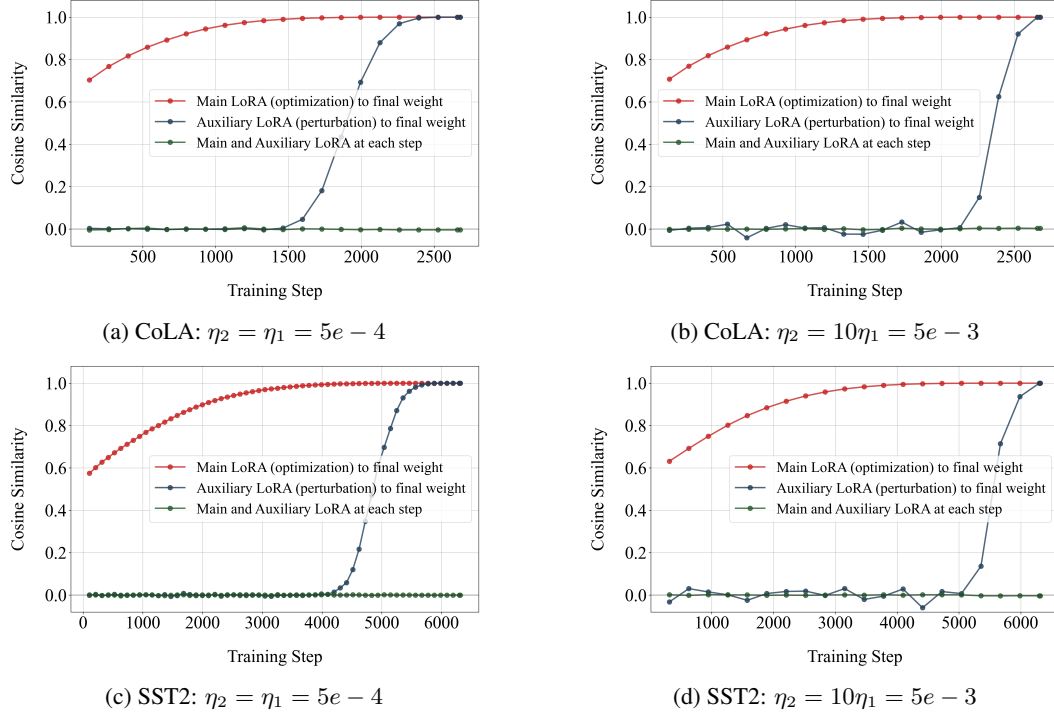


Figure A2: Cosine similarity between the main and auxiliary LoRA weights and each final weights during training on CoLA and SST2 using T5-base, under different auxiliary learning rates (η_2). **The auxiliary module (perturbation, blue lines) converges in the final 20% of steps, significantly slower than the main (optimization, red lines) module.** A larger $\eta_2 = 10\eta_1$ further slows down convergence. Moreover, the auxiliary module’s trajectory remains independent of the main module throughout training (green lines).

D BI-LoRA IN QUANTIZED SETTINGS

We apply Bi-LoRA in a quantized setting, where the transition to lower precision can cause the model to jump from a flat region into a sharper region with higher local loss, reducing generalization on unseen data. Following QLoRA (Dettmers et al., 2023), we quantize the pretrained model to NF4 and adopt the setup described in Section 5.3.

As shown in Table A2, Bi-QLoRA outperforms QLoRA and QLoRA-SAM by 2.58% and 2.36% on GSM8K, respectively. This gain is attributed to Bi-LoRA’s ability to maintain flatness under quantization by decoupling optimization and perturbation during training.

Table A2: Performance on GSM8K under quantized NF4 settings. Results are averaged over 3 runs.

Method	GSM8K (%)
QLoRA	57.77 ± 0.39
QLoRA-SAM	57.89 ± 0.29
Bi-QLoRA	59.26 ± 0.17

E TRAINING AND TEST METRIC CURVES

We fine-tune T5-base on MRPC for 10 epochs, tracking both training and eval losses and metrics. The results in A3 shows nearly identical training losses across methods, yet Bi-LoRA attains a lower validation loss and higher accuracy. Importantly, the smaller train–val generalization gap demonstrates Bi-LoRA’s improved generalization.

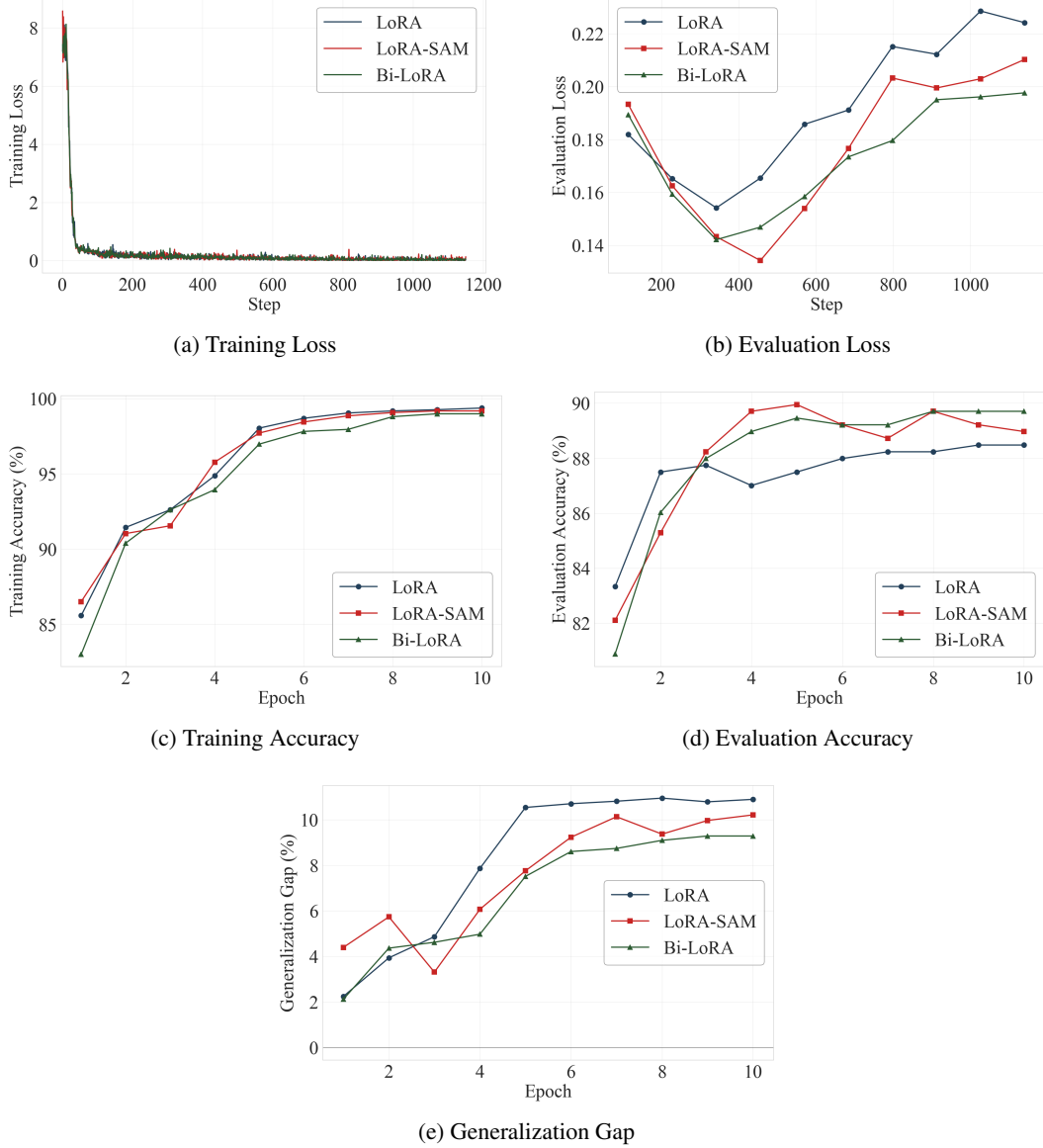


Figure A3: Training and evaluation loss, accuracy, and generalization gap of T5-base fine-tuned on the MRPC dataset.

F COMPUTE RESOURCES

We utilize two types of GPUs: the NVIDIA RTX 4090 24GB and the A100 80GB. All full fine-tuning experiments reported in Section 5.3 and experiments on Llama 3.1-8B are conducted on a single A100. For all other experiments, computations are performed on a single RTX 4090.

G LEARNING RATES FOR TUNING THE TWO MODULES IN BI-LoRA

In our experiments, both modules in Bi-LoRA use the same learning rate of 5×10^{-4} . Initially, we explored an unequal learning rate strategy. However, results in Table A3 show that tuning η_2 provides only a limited improvement in performance. Considering the trade-off between gains and the additional effort for hyperparameter tuning, we recommend using the same learning rate for both modules.

Table A3: CoLA accuracy under different learning rate of the auxiliary module η_2 settings (with $\eta_1 = 5 \times 10^{-4}$ for the main LoRA module).

η_2	1×10^{-4}	5×10^{-4} (main)	5×10^{-3}
CoLA	60.23 \pm 0.35	60.77 \pm 0.55	60.44 \pm 0.87

H EMPIRICAL DETAILS

This section provides detailed empirical setups used for the previous experiments.

H.1 EXPERIMENTS ON THE GLUE AND SUPERGLUE DATASETS

The hyperparameter configurations for all GLUE and SuperGLUE experiments (Sections 5.2, 5.6 and 5.7) are detailed in Tables A4 and A5. As discussed in Section 5.2, we set the neighborhood radius ρ to 0.01 and 0.05 for LoRA-SAM and Bi-LoRA, respectively, in the GLUE experiments. For SuperGLUE, we use ρ values of 0.05 and 0.1 for LoRA-SAM and Bi-LoRA, respectively. For full fine-tuning, we set the learning rate to 1e-4 while keeping all other hyperparameters unchanged. We use the same learning rate of 5e-4 for both the primary and auxiliary LoRA modules in Bi-LoRA.

Table A4: Hyperparameter configurations for fine-tuning T5-base using LoRA-based methods on the GLUE datasets

Hyperparameter	MNLI	SST-2	COLA	QNLI	MRPC
Learning Rate			5e-4		
Batch Size			32		
Epochs	3	3	10	3	10
Max Sequence Length			256		
LoRA Rank			8		
LoRA Alpha			16		
LR Scheduler			Cosine		
Target Modules			All		
Warmup Ratio			0.03		
Evaluation Metric	Accuracy	Accuracy	Matthews Corr.	Accuracy	Accuracy

H.2 EXPERIMENTS ON LARGE LANGUAGE MODELS

The hyperparameter settings for large language models are listed in Tables A6 and A7.

The neighborhood radius ρ is set to 0.01 and 0.1 for LoRA-SAM and Bi-LoRA, except for the instruction following task, where $\rho = 0.05$ for Bi-LoRA to achieve optimal performance. For full fine-tuning, we set the micro-batch size to 4, 2, 2, and 8 for the respective four tasks, and the learning rate is set to 5e-5. We use the same learning rate of 5e-4 for both the primary and auxiliary LoRA modules in Bi-LoRA.

Table A5: Hyperparameter settings for fine-tuning T5-base using LoRA-based methods on the SuperGLUE datasets

Hyperparameter	BoolQ	CB	COPA	RTE	WIC
Learning Rate			5e-4		
Batch Size			32		
Epochs	10	50	50	10	10
Max Sequence Length			256		
LoRA Rank			8		
LoRA Alpha			16		
LR Scheduler			Cosine		
Target Modules			All		
Warmup Ratio			0.03		
Evaluation Metric			Accuracy		

Table A6: Hyperparameter configurations for fine-tuning Llama 2-7B on Math, Code, and Chat tasks using LoRA-based methods. “Math”, “Code” and “Chat” correspond to mathematical reasoning, code generation, and dialogue generation tasks, respectively, as described in Section 5.3.

Hyperparameter	Math	Code	Chat
Learning rate		5e-4	
Batch Size		32	
Micro-Batch size	2	1	1
Epochs		2	
Max Sequence Length		1024	
LoRA Rank		8	
LoRA Dropout		0.0	
LoRA Alpha		16	
Target Modules		All	
LR Scheduler		Cosine	
Warmup Ratio		0.03	

Table A7: Hyperparameter configurations for fine-tuning Llama 3.1-8B on Cleaned Alpaca datasets.

Hyperparameter	Cleaned Alpaca
Learning rate	3e-4
Batch Size	128
Micro-Batch size	4
Epochs	3
Max Sequence Length	256
LoRA Rank	8
LoRA Dropout	0.0
LoRA Alpha	16
Target Modules	All
LR Scheduler	Cosine
Warmup Ratio	0.03

H.3 EXPERIMENTS ON DIFFUSION MODELS

The finetuning dataset, 3D Icons¹, contains 23 training images, all featuring a square icon.

The hyperparameter settings for Diffusion Models are listed in Table A8. We finetune the model for 500 steps with a constant learning rate of $2e-4$, and set the ρ for Bi-LoRA to 0.05. The LoRA rank is set to 4, with an auxiliary rank of 4 for Bi-LoRA. We use the same learning rate of $2e-4$ for both the primary and auxiliary LoRA modules in Bi-LoRA. The instance prompt used for DreamBooth training is “a TOK icon, in the style of TOK”, and the validation prompt used for generating the specific icons is formatted as "a ToK icon of a <Instance>, in the style of ToK". We follow the scripts implemented by Hugging Face².

Table A8: Hyperparameter settings for fine-tuning SDXL using Dreambooth on the 3D Icons dataset

Hyperparameter	Value
Learning Rate	$2e-4$
Batch Size	4
Micro-Batch Size	1
Train Steps	500
Resolution	1024
Validation Epochs	25
LoRA Rank r	4
LoRA Dropout	0.0
LoRA Alpha α	8
Target Modules	W_K, W_Q, W_V, W_O
LR Scheduler	Constant
Warmup Steps	0

H.4 EFFICIENT SAM VARIANTS FOR LoRA FINE-TUNING

To ensure a fair comparison, we adopt the results of Flat-LoRA from Li et al. (2024b), and follow the default setup of Li et al. (2024a) for LoRA-oBAR/nBAR with $\alpha = 0.25$. All other hyperparameters are aligned with those used in our prior experiments.

I TIME COMPARISONS ACROSS TASKS

In this section, we compare the per-step optimization time for LoRA, LoRA-SAM, and Bi-LoRA across a range of benchmarks. The results are organized based on different datasets and tasks, including T5 experiments on the GLUE and SuperGLUE datasets, as well as Llama experiments on domain-specific datasets. All experiments were conducted on a single NVIDIA RTX 4090 GPU 24GB, using the same hyperparameters as in the previous experiments.

Table A9: Optimization time (s) per step for T5-base on GLUE benchmarks. The average time across tasks is also reported.

Dataset	MNLI	SST2	CoLA	QNLI	MRPC	Avg. Time
Full FT	0.758	0.538	0.549	0.756	0.681	0.654
LoRA	0.458	0.310	0.273	0.508	0.442	0.398
LoRA-SAM	1.036	0.573	0.546	0.950	1.039	0.829
Bi-LoRA	0.476	0.325	0.305	0.513	0.508	0.425

¹https://huggingface.co/datasets/linoyts/3d_icon

²https://github.com/huggingface/diffusers/blob/main/examples/dreambooth/README_sdxl.md

Table A10: Optimization time (s) per step for T5-base on SuperGLUE benchmarks. The average time across tasks is also reported.

Dataset	BoolQ	CB	COPA	RTE	WIC	Avg. Time
Full FT	0.622	0.415	0.451	0.689	0.544	0.544
LoRA	0.276	0.276	0.253	0.263	0.286	0.271
LoRA-SAM	0.519	0.534	0.568	0.688	0.484	0.559
Bi-LoRA	0.304	0.285	0.278	0.276	0.262	0.281

Table A11: Optimization time (s) per step for training Llama2 on math (MetaMathQA), code (Code-Feedback) and chat (WizardLM) tasks.

Dataset	MetaMathQA	Code-Feedback	WizardLM
LoRA	4.337	7.784	7.942
LoRA-SAM	9.350	16.871	16.993
Bi-LoRA	4.501	7.884	8.199

J NORM AND RATIO ANALYSIS ACROSS LAYERS

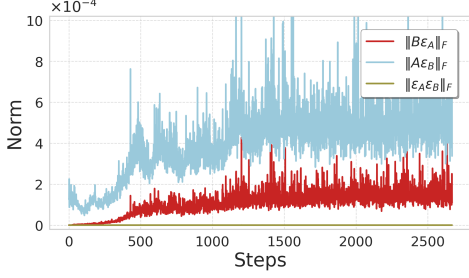
In addition to Figures 2a and 2b, we extend the analysis of LoRA-SAM’s training dynamics to additional self-attention layers across different encoder blocks to verify the consistency of our observations.

Figures A4a, A4c and A4e show the Frobenius norms of different terms in the key, output projection and value of self-attention layers in the 5th, 8th, and 9th encoder blocks, respectively. And Figures A4b, A4d and A4f present corresponding norm ratios. As observed, the norm of the third higher-order term remains several orders of magnitude smaller than the first two terms, confirming its negligible impact.

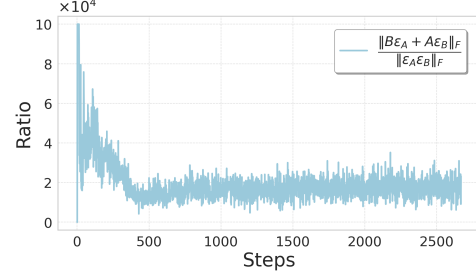
K BROADER IMPACTS AND LIMITATIONS

Broader Impacts. Bi-LoRA jointly trains primary and adversarial auxiliary LoRA modules within a low-rank adaptation framework, introducing SAM-style perturbations in a parameter-efficient manner. This design cuts the memory and energy footprint of sharpness-aware fine-tuning for large language models while improving downstream generalization. By lowering the hardware barrier, Bi-LoRA democratizes LLM research and empowers resource-constrained laboratories. However, the technique could also enable malicious actors to rapidly customize harmful models or inadvertently amplify dataset biases. Moreover, the gradient-ascent auxiliary adapter—though beneficial for robustness—creates an additional attack surface that might be exploited to implant backdoors or trigger uncontrolled behaviors.

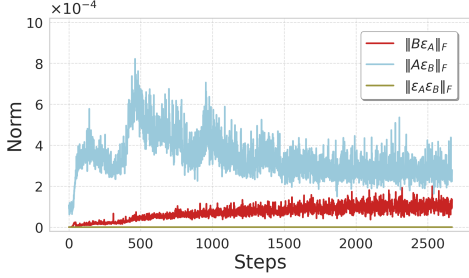
Limitations. Bi-LoRA achieves promising gains in parameter-efficient fine-tuning and improved downstream generalization, but it has limitations as follows: (i) Constrained by compute, we evaluate only on Llama 2-7B and Llama 3.1-8B, leaving larger or multimodal models unexplored. (ii) Although Bi-LoRA appears to find flatter minima in the full parameter space, this evidence is empirical only and lacks a formal generalization proof. (iii) We focus on addressing the specific shortcoming of LoRA-SAM, i.e., its adversarial perturbations are restricted to the LoRA optimization subspace rather than the full weight space; we have not explored how Bi-LoRA interacts with other SAM variants, which we leave for future work.



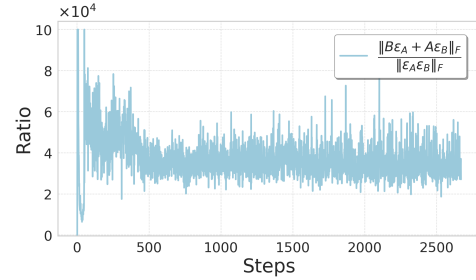
(a) Norm of different components in the key of the first self-attention layer in the fifth encoder block



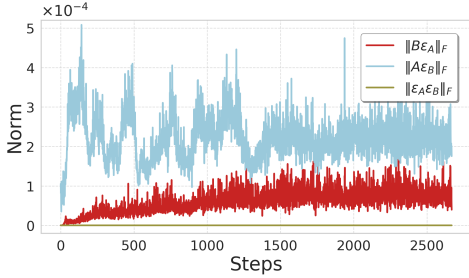
(b) Norm ratio of the key of the first self-attention layer in the fifth encoder block



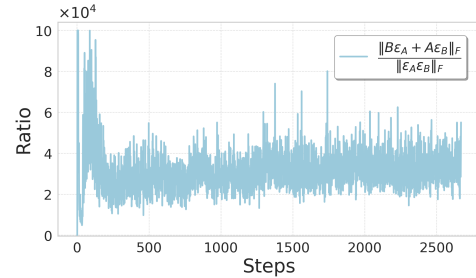
(c) Norm of different components in the output projection the second self-attention layer in the eighth encoder block



(d) Norm ratio of the output projection in the second self-attention layer in the eighth encoder block



(e) Norm of different components in the value of the first self-attention layer in the ninth encoder block



(f) Norm ratio of the value of the first self-attention layer in the ninth encoder block

Figure A4: Analyses of training statistics for LoRA-SAM. (a) and (c) and (e): Frobenius norms of different terms. And (b), (d) and (f): ratio of the Frobenius norms of the first two terms ($B\epsilon_A + \epsilon_B A$) to that of the third term ($\epsilon_B \epsilon_A$) in Eqn. (5) during fine-tuning. Models are fine-tuned on CoLA with T5 for 10 epochs.